Short title: Systemic regulation in a rhizomatous wild rice

Author for contact details: Hitoshi Sakakibara (sakaki@agr.nagoya-u.ac.jp)

Systemic regulation of nitrogen acquisition and use in *Oryza longistaminata* ramets under nitrogen heterogeneity[1]

Misato Kawai[a], Ryo Tabata[a], Miwa Ohashi[a], Haruno Honda[a], Takehiro Kamiya[b], Mikiko Kojima[c], Yumiko Takebayashi[c], Shunsuke Oishi[d], Satoru Okamoto[a,e], Takushi Hachiya[a,f], Hitoshi Sakakibara[a,c,2,3]

[a]Graduate School of Bioagricultural Sciences, Nagoya University, Chikusa, Nagoya 464-8601, Japan

[b]Graduate School of Agricultural and Life Sciences, The University of Tokyo, Bunkyo, Tokyo 113-8657, Japan

[c]RIKEN Center for Sustainable Resource Science, Tsurumi, Yokohama 230-0045, Japan

[d]Institute of Transformative Bio-Molecules (WPI-ITbM), Nagoya University, Chikusa, Nagoya 464-8602, Japan

[e]Graduate School of Science and Technology, Niigata University, Niigata 950-2181, Japan

[f]Department of Molecular and Function Genomics, Interdisciplinary Center for Science Research, Shimane University, Matsue, 690-8504, Japan

One sentence summary: *Oryza longistaminata*, a rhizomatous wild rice, systemically regulates nitrogen acquisition and use in response to spatially heterogeneous nitrogen availability via inter-ramet communication.

Footnotes:

Author Contributions: M.Ka., H.H., M.O., S.Ok., T.H. and H.S. designed the experiments and analyzed the data; M.Ka. and H.H. performed all experiments and M.O., S.Ok., T.H., and H.S. supervised M.Ka. and H.H.; R.T. and T.K. helped with RNAseq data analysis; M.Ko. and Y.K. provided technical support to quantify cytokinins; S.Oi. synthesized CEP peptides; H.S.

conceived the project and wrote the manuscript with contributions from all co-authors; H.S. agrees to serve as the author responsible for contact and ensures communication.

Funding:

[1]This research was supported by the Advanced Low Carbon Technology Research and Development Program from the Core Research for Evolutional Science and Technology (to H.S.; no. JPMJCR13B1), PRESTO (to S.Ok.; no. JPMJPR17Q2) by JST, Leading Initiative for Excellent Young Researchers (to S.Ok.), Grants-in-Aid from the Ministry of Education, Culture, Sports, Science and Technology, Japan (to H.S.; 17H06473 and 19H00931, to R.T.; 18K05373 and 20H05501, to T.K.; 17H03782), and by the Program for Promoting the Enhancement of Research Universities, Nagoya University.

[2]Author for contact: sakaki@agr.nagoya-u.ac.jp.

[3]Senior author.

Abstract

Oryza longistaminata, a wild rice, vegetatively reproduces and forms a networked clonal colony consisting of ramets connected by rhizomes. Although water, nutrients, and other molecules can be transferred between ramets via the rhizomes, inter-ramet communication in response to spatially heterogeneous nitrogen availability is not well understood. We studied the response of ramet pairs to heterogeneous nitrogen availability by using a split hydroponic system that allowed each ramet root to be exposed to different conditions. Ammonium uptake was compensatively enhanced in the sufficient-side root when roots of the ramet pairs were exposed to ammonium-sufficient and deficient conditions. Comparative transcriptome analysis revealed that a gene regulatory network for effective ammonium assimilation and amino acid biosynthesis was activated in the sufficient-side roots. Allocation of absorbed nitrogen from the nitrogen-sufficient to the deficient ramets was rather limited. Nitrogen was preferentially used for newly growing axillary buds on the sufficient-side ramets. Biosynthesis of *trans*-zeatin, a cytokinin, was up-regulated in response to the nitrogen supply, but *trans*-zeatin appears not to target the compensatory regulation. Our results also implied that the *O. longistaminata* ortholog of *OsCEP1* plays a role as a nitrogen-deficient signal in inter-ramet communication, providing

compensatory up-regulation of nitrogen assimilatory genes. These results provide insights into the molecular basis for efficient growth strategies of asexually proliferating plants growing in areas where nitrogen distribution is spatially heterogeneous.

Introduction

Oryza longistaminata is a wild rice species that preferentially grows in wetlands and vegetatively reproduces through rhizome growth that can be so vigorous as to occupy an area completely (Vaughan, 1994). Rhizome growth is characterized by the underground horizontal outgrowth of axillary buds to form new rhizomes that expand into new territory (Yoshida et al., 2016; Fan et al., 2017; Kyozuka, 2017; Bessho-Uehara et al., 2018; Toriba et al., 2020; Shibasaki et al., 2021). Rhizome tips developmentally transform into photosynthetic above-ground organs by growing into a new plantlet called a ramet. Continuous rhizome growth and subsequent transformation form a networked clonal colony. In addition to *O. longistaminata*, many other plant species vegetatively reproduce through rhizome growth, such as *Phyllostachys edulis* (Moso bamboo) and *Zoysia matrella* (Manila grass)(Guo et al., 2021), and show vigorous fertility. Since ramets are connected via rhizomes, water, nutrients, and other molecules can be transferred between ramets (De Kroon et al., 1998). Therefore, the growth and metabolism of a ramet are not totally independent of the neighboring ramets but have some influence on each other via the rhizomes.

Nitrogen is one of the most limiting macronutrients for plants, so nitrogen acquisition and use efficiency significantly affect plant growth and development. In submerged and reductive soil conditions where wetland rice grows, plants mainly use ammonium ions as the inorganic nitrogen source (Yoshida, 1981). In *Oryza sativa*, ammonium ions in the soil are taken up by ammonium transporters (AMTs)(Sonoda et al., 2003; Suenaga et al., 2003; Yuan et al., 2007; Li et al., 2016; Jia and von Wirén, 2020; Lee et al., 2020a), and then are initially assimilated into glutamine and glutamate by the glutamine synthetase (GS)/ glutamate synthetase (GOGAT) cycle (Lea and Miflin, 1974). The cycle is mainly composed of cytosolic GS and plastidic NADH-GOGAT isoforms in the root (Ishiyama et al., 2004; Tabuchi et al., 2005; Tabuchi et al., 2007; Funayama et al., 2013; Yamaya and Kusano, 2014; Ji et al., 2019; Lee et al., 2020b). Several amino acids are synthesized by amino-transfer reactions from glutamine and glutamate to

organic acids derived from glycolysis, the tricarboxylic acid cycle, and the pentose phosphate pathway. Previous studies using *O. sativa*, *Arabidopsis thaliana*, and *Nicotiana tabacum* revealed a wide and versatile regulatory network of gene expression in response to nitrogen (nitrate or ammonium) nutrition, including genes for the processes of uptake, assimilation, amino acid synthesis, carbon skeleton supply, and hormone signaling (Scheible et al., 1997; Scheible et al., 2004; Wang et al., 2004; Sakakibara et al., 2006; Chandran et al., 2016; Yang et al., 2017; Sun et al., 2020).

Plants optimize their growth and development according to the amount of available nitrogen, and signaling molecules, including phytohormones and peptide hormones, play a key role in this regulation (Nishida and Suzaki, 2018; Ruffel, 2018; Sakakibara, 2021; Wheeldon and Bennett, 2021). Cytokinin, especially *trans*-zeatin (tZ), promotes nitrogen-responsive shoot growth via modulating shoot meristem activity (Kiba et al., 2013; Davière and Achard, 2017; Osugi et al., 2017; Landrein et al., 2018). An abundant nitrate supply promotes *de novo* tZ biosynthesis via the up-regulation of *ADENOSINE PHOSPHATE-ISOPENTENYLTRANSFERASE3* (*IPT3*) and *CYP735A2* in Arabidopsis (Takei et al., 2004; Maeda et al., 2018; Naulin et al., 2019; Sakakibara, 2021). In *O. sativa*, a glutamine-related signal stimulates *OsIPT4* and *OsIPT5* expression that are involved in axillary bud outgrowth from shoots (Kamada-Nobusada et al., 2013; Ohashi et al., 2017). In *O. longistaminata*, the outgrowth of rhizome axillary buds in response to nitrogen nutrition is regulated by a similar process to that of the axillary shoot bud in *O. sativa*, despite differences in the physiological roles of these organs (Shibasaki et al., 2021). In contrast, strigolactone is involved in the nutrient-responsive suppression of shoot axillary bud outgrowth (Gomez-Roldan et al., 2008; Umehara et al., 2008; Minakuchi et al., 2010; Umehara et al., 2010). Strigolactone biosynthetic genes are known to be up-regulated in the roots of *O. sativa* and *Zea mays* under nitrogen-deficient (Sun et al., 2014; Xu et al., 2015; Ravazzolo et al., 2019; Ravazzolo et al., 2021) and phosphorus-deficient (Umehara et al., 2010) conditions.

It is essential for plants to efficiently acquire nutrients for optimal growth and development even though mineral nutrients are heterogeneously distributed in the soil. Recent studies using a split-root system in Arabidopsis showed that when part of the root system is subjected to nitrogen deficiency, C-TERMINALLY ENCODED PEPTIDE1 (CEP1), synthesized in the deficient root, is translocated to shoots via the xylem (Ohyama et al., 2008; Tabata et al., 2014). The perception of CEP1 by the CEP1 RECEPTOR (CEPR) in shoots triggers the expression of

124 CEP DOWNSTREAM (CEPD) proteins that are translocated to the root system via the phloem,
125 thereby promoting compensatory nitrogen uptake by inducing the expression of high-affinity
126 nitrate transporters, including *NITRATE TRANSPORTER2.1* (*NRT2.1*) in the nitrogen-ample
127 side (Tabata et al., 2014; Okamoto et al., 2016; Ohkubo et al., 2017; Ruffel and Gojon, 2017;
128 Ota et al., 2020; Ohkubo et al., 2021). In rhizomatous plants, ramets connected by rhizomes are
129 regarded as one individual; however, it remains unknown whether each ramet responds to
130 nitrogen availability independently or compensatively when growing in areas where nitrogen
131 distribution is spatially heterogeneous.
132 In this study, we characterized the response of *O. longistaminata* ramet pairs, connected by a
133 rhizome, to spatially heterogeneous nitrogen conditions and found a compensatory gene
134 regulatory network for effective acquisition and assimilation of nitrogen in the ample-side ramet
135 root. Cytokinin biosynthesis was up-regulated in response to nitrogen supply, but this increase
136 appears to be independent of the compensatory regulation. Our results also imply that an *O.*
137 *longistaminata* ortholog of the *OsCEP1* gene plays a role in inter-ramet communication. This
138 study provides valuable hints for understanding the molecular basis of efficient growth strategies
139 of vegetatively proliferating plants.
140
141 **Results**
142 **Compensatory promotion of ammonium uptake in response to a spatially heterogeneous**
143 **nitrogen supply in *O. longistaminata* ramet pairs**
144 To examine nitrogen-related inter-ramet communication via the rhizome, we established a
145 split-hydroponic experimental system for *O. longistaminata* ramet pairs (Supplemental Fig. S1).
146 After preparing young ramet pairs of comparable growth stages that developed at adjacent
147 rhizome nodes, we treated the roots of each ramet to different levels of nitrogen nutrition to
148 mimic a condition of spatially heterogeneous nitrogen availability. We set up three conditions: (i)
149 both ramet roots were exposed to 2.5 mM NH_4Cl (+N), (ii) one ramet root was exposed to 2.5
150 mM NH_4Cl (+N split), and the other was exposed to 0 mM NH_4Cl (-N split), (iii) both ramet roots
151 were exposed to 0 mM NH_4Cl (-N) (Fig. 1A and Supplemental Fig. S1F). We compared the
152 absorption activity of ammonium between the +N and +N split roots using ^{15}N-labeled NH_4Cl as
153 the tracer. The results showed that the ammonium absorption activity was significantly
154 increased by about 1.6-fold in the +N split ramets compared to the +N ramets (Fig. 1B).

155 Expression of the *OlAMT1;2* gene, an ortholog of *O. sativa AMT1;2* that encodes an
156 ammonium-inducible ammonium transporter, was approximately 3.6-fold higher in the roots of
157 +N split than those of +N (Fig. 1C). These results suggest that when *O. longistaminata* ramet
158 pairs are exposed to nitrogen that is spatially heterogeneous, ammonium uptake is
159 compensatively enhanced in the ramet exposed to the nitrogen-rich condition and is
160 accompanied by an up-regulation of *OlAMT1;2*.
161
162 **Compensatory regulation of amino acid biosynthesis and related genes in response to a**
163 **spatially heterogeneous nitrogen supply**
164 To explore the molecular basis underlying the compensatory response to a heterogeneous
165 nitrogen supply, we analyzed the transcriptome using RNA sequencing (RNAseq) of the roots at
166 24 h after the start of the +N, +N split, -N split, and -N treatments. Up- and down-regulated
167 genes were identified from the expression data of the +N split, -N split, and -N treatments by
168 comparison with that of the +N condition (false discovery rate [FDR] < 0.05). In comparison to
169 the +N condition, 416 genes were significantly up-regulated in +N split root (Figs. 2A and 2B,
170 Supplemental Table S1). Also, 2361 and 2776 genes were up-regulated in +N roots compared
171 to the -N and -N split treatments, respectively (Fig. 2B, Supplemental Tables S2 and S3).
172 Among the 416 genes, the identity of 295 genes overlapped with both the up-regulated genes in
173 the +N treatment compared to the -N treatment and those in the +N treatment compared to the -
174 N split treatment (110 genes), or only with those in the +N treatment compared to the -N split
175 treatment (179 genes) and to the -N treatment (6 genes) (Fig. 2B). Gene Ontology (GO)
176 analysis showed that genes associated with metabolic processes related to nitrogen and
177 carbon, such as glycolysis (p = 2.7e-8), monosaccharide metabolic processes (p = 1.8e-7),
178 oxoacid metabolic processes (p = 3.5e-7), and cellular amino acid metabolic processes (4.6e-
179 6), were enriched among the 416 genes (Fig. 2C). Specifically, the up-regulated genes included
180 those involved in nitrogen assimilation and amino acid synthesis, such as genes for a cytosolic
181 glutamine synthetase *OlGS1;2*, an NADH-dependent glutamate synthase *OlNADH-GOGAT2*,
182 an aspartate aminotransferase *OlAspAT*, an aspartate semialdehyde dehydrogenase
183 *OlASADH*, an aspartate kinase-homoserine dehydrogenase *OlAK-HSDH1*, an alanine
184 aminotransferase *OlAlaAT1*, and an aspartate kinase *OlAK* (Supplemental Table S1). Using
185 reverse transcription-quantitative PCR (RT-qPCR), we confirmed that these genes were

186 significantly up-regulated in +N split roots compared to +N (Fig. 3B). In addition, the expression
187 of glycolytic enzyme genes involved in supplying carbon skeletons for amino acid biosynthesis,
188 such as glucose-6-phosphate isomerase (*OlGPI*), triosephosphate isomerase (*OlTPI1*), fructose
189 1,6-bisphosphate aldolase (*OlALDC1*), glyceraldehyde 3-phosphate dehydrogenase
190 (*OlGAPC1*), phosphofructokinase (*OlPFK5*), enolase (*OlENO1*), a glycolysis-related pyruvate
191 orthophosphate dikinase (*OlPPDKA*), and phosphoenolpyruvate carboxylase (*OlPPC4*) were
192 also significantly up-regulated in the +N split root condition compared to the +N treatment (Fig.
193 3A、Supplemental Table S1). These results suggest that a compensatory gene regulatory
194 network to acquire and assimilate ammonium effectively is activated in the ramet roots on the
195 nitrogen-sufficient side of the ramet pairs.
196 To know the impact of transcriptome changes on the accumulation level of amino acids, we
197 analyzed the amino acid concentrations in roots from the +N, +N split, -N split, and -N
198 treatments at a longer treatment period (48 h). As a result, the accumulation level of glutamine,
199 asparagine, aspartate, alanine, glutamate, and arginine were significantly higher in the +N split
200 roots than in the -N split roots (Fig. 3C). Among these amino acids, aspartate and alanine levels
201 in roots from the +N split treatment were significantly higher than those in the +N treatment.
202 Other amino acids except for arginine showed a similar tendency. These results are in line with
203 the transcriptome changes in response to heterogeneous nitrogen availability.
204 On the other hand, 1848 and 2087 genes were up-regulated in the -N and -N split treatments
205 compared to the +N condition, respectively (Supplemental Table S4 and S5). Overall, the
206 expression of 1176 genes overlapped between the two conditions (Supplemental Fig. S2). One
207 hundred and forty-five genes were up-regulated in the +N treatment compared to the +N split
208 treatment (Supplemental Table S6), and 15 genes overlapped with the -N-up-regulated genes
209 (Supplemental Fig. S2).
210
211 **Allocation of absorbed nitrogen between ramets via the rhizome when nitrogen**
212 **availability is spatially heterogeneous**
213 To examine the allocation of absorbed nitrogen in ramet pairs when nitrogen availability is
214 spatially different, $^{15}NH_4Cl$ was fed to +N and +N split roots with the same conditions as shown
215 in Fig. 1B, and the roots were grown for another 7 days with a non-labeled nitrogen source. In
216 this experimental condition, ^{15}N was detected in both the shoots and roots of the systemic +N

217 and -N split ramets that had not been fed with $^{15}NH_4Cl$ (Fig. 4A), indicating that absorbed
218 nitrogen is allocated to neighboring ramets via the rhizome. The percentage distribution of ^{15}N
219 was higher in the shoots than in the roots. Interestingly, the allocation of absorbed nitrogen from
220 the +N split to the -N split ramets was less than that from the +N to the +N ramets.
221
222 **Growth response of ramets in spatially heterogeneous nitrogen conditions**
223 To know the long-term effects of nitrogen split treatment on the growth of ramets, we
224 exposed ramet pairs to different nitrogen conditions for 5 weeks, and growth parameters for
225 each ramet were monitored (Figs. 4B to E). Plant height, the number of fully developed leaves,
226 chlorophyll content, and the number of growing axillary buds were significantly higher in the +N
227 and +N split ramets than in the -N split and -N ramets. The chlorophyll content was lower in the
228 -N split and -N ramet shoots, but the decrease was significantly alleviated in the -N split ramets
229 compared to the -N ramets (Fig. 4D), suggesting that the allocated nitrogen was used to retain
230 photosynthetic function. In contrast, the change in the number of growing axillary buds was
231 almost zero for the -N and -N split ramets, whereas the axillary bud number increased
232 significantly in the +N split and +N ramets (Fig. 4E). In particular, the axillary bud number was
233 significantly higher in the +N split ramets than in the +N ramets. These results suggest that
234 when neighboring ramets are exposed to different levels of nitrogen availability, the allocation of
235 absorbed nitrogen from the N-sufficient ramet to the deficient ramet is rather limited and,
236 nitrogen is preferentially allocated for newly growing axillary buds.
237
238 **Response of cytokinin and strigolactone biosynthetic genes in response to a**
239 **heterogeneous nitrogen supply**
240 To gain insight into the growth promotion of axillary buds in the +N split ramets, we focused
241 on cytokinin and strigolactone, two phytohormone families that promote and inhibit axillary bud
242 outgrowth, respectively. We analyzed the expression levels of cytokinin and strigolactone
243 biosynthetic genes by RT-qPCR using the roots of ramet pairs that had been split-treated for 7
244 days. The expression levels of cytokinin biosynthetic genes, *OlIPT4*, *OlIPT5*, *OlCYP735A3*, and
245 *OlCYP735A4* were higher in the roots of the +N and +N split ramets than in those of the -N and
246 -N split ramets (Fig. 5A), and there was no difference between the +N and +N split conditions.

247 We also analyzed the concentration of cytokinins in the roots. The level of *trans*-zeatin (tZ)-
248 type cytokinins, including the riboside and ribotide precursors, was higher in the +N and +N split
249 roots compared to the -N split and -N roots, whereas the levels of N^6-(Δ^2-isopentenyl)adenine
250 (iP)-type cytokinins were somewhat lower (Fig. 5B, Supplemental Table S7). The tZ-type
251 cytokinin content in the +N and +N split roots was comparable, suggesting that de novo tZ-type
252 cytokinin biosynthesis is enhanced in response to nitrogen supply but is not under the
253 compensatory regulation.
254 Although strigolactone species in *O. longistaminata* have not been well characterized yet, we
255 analyzed orthologs of *O. sativa D27*, *D17*, and *D10* (*OlD27*, *OlD17*, and *OlD10*, respectively)
256 encoding enzymes involved in the production of carlactone, an intermediate of strigolactone
257 biosynthesis (Alder et al., 2012). The expression level of *OlD10* was significantly higher in -N
258 ramet roots than in other conditions, although *OlD27* and *OlD17* expression levels were
259 essentially similar and slightly lower, respectively (Fig. 5C). This result implies that de novo
260 strigolactone biosynthesis might be up-regulated in nitrogen-deficient roots.
261
262 **Possible involvement of a CEP1-type peptide in inter-ramet nitrogen-deficiency signaling**
263 In Arabidopsis, CEP1 plays a key role in the systemic regulation of nitrate acquisition in
264 response to heterogeneous nitrogen conditions as a root-to-shoot signaling molecule (Tabata et
265 al., 2014; Okamoto et al., 2016). To investigate whether a CEP1-type peptide is involved in the
266 observed inter-ramet communication, we analyzed the response of *O. longistaminata* CEP gene
267 orthologs to spatially heterogeneous nitrogen availability. In *O. sativa*, 15 genes encode CEPs
268 (Sui et al., 2016). We searched for the orthologs in *O. longistaminata* and found 15 sequences
269 corresponding to each of the *O. sativa* genes (Supplemental Table S8), and eight of the genes
270 (*OlCEP5*, *OlCEP6.1*, *OlCEP9*, *OlCEP10*, *OlCEP11*, *OlCEP12*, *OlCEP14*, and *OlCEP15*) were
271 annotated in our RNAseq data. However, expression of these eight genes was not significantly
272 different in -N roots compared to +N roots. Next, we focused on *OlCEP1* and analyzed its
273 expression level by RT-qPCR because the peptide sequences encoded by *OsCEP1* (also
274 *OlCEP1*) belong to the same group (group I) as Arabidopsis CEP1 based on the structural
275 features (Delay et al., 2013; Sui et al., 2016). In the RT-qPCR analysis, the expression level of
276 *OlCEP1* in -N roots was significantly higher than in the +N and +N split roots (Fig. 6A).

277 To gain further insight into the involvement of *OlCEP1* gene products in nitrogen-related
278 ramet-to-ramet signaling, we examined the effect of an exogenous application of OlCEP1
279 peptides on the expression of *OlAMT1;2* and *OlGS1;2* genes. In addition to *OsCEP1*, the
280 coding sequence of the *OlCEP1* gene contains multiple CEP sequences containing proline
281 residues. Thus, we synthesized peptides OlCEP1a to OlCEP1d (See Materials and Methods)
282 and used a mixture. We treated ramet roots with the peptide mixture under nitrogen-sufficient
283 conditions to repress the endogenous *OlCEP1* expression. When we applied OlCEP1 peptides
284 to the roots of one side of the ramets, the accumulation level of transcripts for *OlAMT1;2* and
285 *OlGS1;2* increased in both the local side and systemic side of the ramet roots in 6 h. The
286 transcript level significance was maintained in the systemic side of the root even at 24 h after
287 treatment (Fig. 6B), suggesting that CEP1-related signaling is possibly involved in the systemic
288 regulation of the genes via the rhizomes.
289
290 **Discussion**
291 In this study, we demonstrated inter-ramet communication occurs in *O. longistaminata* via
292 rhizomes for a systemic response to spatially heterogeneous nitrogen availability. When ramet
293 pairs of *O. longistaminata* connected by a rhizome were exposed to different nitrogen nutrient
294 conditions, a series of gene networks that allow complementary absorption and assimilation of
295 ammonium was activated in the root of the ramet in the nitrogen-sufficient condition. This
296 network also included genes capable of supplying the carbon skeletons for amino acid
297 synthesis, such as those involved in glycolysis. The expression level of these genes in the
298 nitrogen-sufficient side of the heterogeneous condition was higher than in the nitrogen
299 homogeneously sufficient condition, suggesting that the nitrogen-deficient side ramet conveyed
300 some kind of nitrogen deficiency signal to the sufficient side ramet via the rhizome to trigger the
301 systemic response.
302 In our transcriptome analysis, a large part of the compensatively up-regulated genes
303 overlapped with ammonium-responsive genes (295 genes/416 genes, Fig. 2B), indicating that
304 the expression of the compensatory genes is up-regulated by an ammonium-signal *per se* but
305 further boosted by the input of a systemic nitrogen-deficient signal from the adjacent ramet. It is
306 not clear at present whether a de-repression or a more facilitative regulatory event underlies the
307 process.

308 A small part of the nitrogen absorbed in the ramet roots in the heterogeneous nitrogen-
309 sufficient condition (+N split) was distributed to the adjacent nitrogen-deficient ramets (-N split),
310 contributing to the maintenance of the chlorophyll content. However, no evidence was obtained
311 to suggest that the distributed nitrogen was used for growth of the nitrogen-deficient side ramet.
312 In a previous study in *Carex flacca* examining water and nitrogen transfer between ramets via
313 the rhizome, the direction of nitrogen nutrient transport depended on the direction of water
314 transport (De Kroon et al., 1998). In rice cultivars, the nitrogen-sufficient condition elevates the
315 leaf transpiration rate compared to the limited condition (Xiong et al., 2015). Thus, it is likely that
316 the translocation of nitrogen from the sufficient side to the deficient side against the water flow is
317 limited between rhizome-connected ramets experiencing different nitrogen conditions. Our
318 results suggest that most compensatively acquired nitrogen is locally used for growth on the
319 sufficient side. Given that an *O. longistaminata* cluster is a single clonal colony, this use of
320 nitrogen might be a strategy to ensure the colony's survival in limited and heterogeneous
321 nitrogen conditions.
322 Notably, genes for the biosynthesis of tZ-type cytokinins, *IPTs* and *CYP735As*, were up-
323 regulated by the nitrogen supply. Still, the expression levels and accumulation of tZ-type
324 cytokinins (tZ and its precursors) were comparable between the +N and +N split treatments in
325 our experiments (Fig. 5B). Therefore, we hypothesize that cytokinin synthesis is similarly up-
326 regulated in response to both homogeneous and heterogeneous nitrogen conditions.
327 Ammonium acquisition and amino acid synthesis, however, are compensatively enhanced in the
328 nitrogen-rich ramet roots under heterogeneous conditions, resulting in a greater supply of
329 nitrogen assimilates for axillary bud outgrowth. Both the cytokinin signal and the supply of
330 building blocks could contribute to the preferential axillary shoot growth.
331 In our analysis, iP and its precursors were in low abundance in the +N and +N split roots,
332 mainly due to the decreased levels of its ribotide precursor (iPRPs, Fig. 5B). At present, we do
333 not have a clear explanation for the opposite trend despite the up-regulation of its biosynthetic
334 genes, *OlIPTs*. The iP ribotide precursor might be over consumed by CYP735As to produce tZ-
335 type species.
336 Previous studies in *O. sativa* and *O. longistaminata* indicated that *NADH-GOGAT1* is under
337 the same control as *IPT4* in the local nitrogen response and that glutamine-related signaling is
338 involved in the regulation (Kamada-Nobusada et al., 2013; Ohashi et al., 2017; Shibasaki et al.,

339 2021). *OlNADH-GOGAT2*, an isogene, is compensatively up-regulated in our experimental
340 conditions, whereas *OlNADH-GOGAT1* had a similar expression pattern to *OlIPT4*
341 (Supplemental Fig. S3). In *O. sativa*, *NADH-GOGAT2* is mainly expressed in mature leaves and
342 plays a role in providing glutamate for the GS1;1 reaction in vascular tissues for nitrogen
343 remobilization and recycling (Tabuchi et al., 2005; Tabuchi et al., 2007; Yamaya and Kusano,
344 2014). Our RNAseq data show that *OlGS1;1* is up-regulated in nitrogen-deficient conditions
345 (Supplemental Tables S4 and S5) in a manner distinct from *OlNADH-GOGAT2*. Thus, the
346 physiological role of the cytosolic GS isoforms and NADH-GOGAT isoforms might be different
347 between *O. sativa* and *O. longistaminata*.
348 Systemic regulation of nitrate acquisition in response to heterogeneous nitrogen nutrient
349 conditions by CEP1-CEPR-CEPD has been identified in Arabidopsis (Tabata et al., 2014;
350 Okamoto et al., 2016; Ohkubo et al., 2017; Ruffel and Gojon, 2017; Ota et al., 2020; Ohkubo et
351 al., 2021). In our analysis, the *O. longistaminata* ortholog of *OsCEP1* was markedly induced by
352 nitrogen deprivation, and exogenous application of the synthetic CEP1 peptides increased the
353 expression level of *OlAMT1;2* and *OlGS1;2* on the systemic side as well as the local side. This
354 finding implies that CEP plays a role in inter-ramet communication as a nitrogen-deficient
355 signaling molecule via the rhizome. Also, our results suggest that both the CEP-derived signal
356 and nitrogen sufficiency are necessary to drive the compensatory up-regulation system, as is
357 the case for *NRT2.1* up-regulation in Arabidopsis (Tabata et al., 2014). The systemic response
358 mechanism responding to heterogeneous nitrogen conditions in monocots, including rice, is still
359 largely unexplored. Identifying and characterizing the CEP receptor and downstream factors,
360 including CEPD orthologs in *O. longistaminata*, is necessary to understand entirely the whole
361 system at the molecular level. The findings of this study will be useful in characterizing survival
362 strategies of rhizomatous plants in response to heterogeneous nitrogen environments.
363
364 **Materials and methods**
365 **Plant materials and growth conditions**
366 The perennial wild rice species *O. longistaminata* (IRGC10404) was hydroponically grown
367 under natural light conditions in a greenhouse with a nutrient solution described by Kamachi et
368 al. (1991), except that the solution contained 1 mM NH_4Cl as the sole nitrogen source and was
369 renewed once every 3 or 4 days. Pairs of young ramets grown on the proximal nodes of

370 rhizomes were excised and used in experiments. The growth stage of all ramet pairs was
371 similar; each ramet had two to three fully developed leaves (Supplemental Fig. S1).
372
373 **Split treatment**
374 The roots of each ramet pair, connected by rhizomes, were incubated in two separate pots
375 (Supplemental Fig. S1). One L of nutrient solution was used for each ramet. For the ±N split
376 treatment, one of the ramet pairs was treated with the nutrient solution containing 2.5 mM NH_4Cl
377 (+N split), and the other was treated with 0 mM NH_4Cl (-N split). For comparison, both ramet
378 pairs were treated with 2.5 mM NH_4Cl (+N) or 0 mM NH_4Cl (-N). Treatments for the growth
379 analysis, and cytokinin and strigolactone response analysis were conducted in a greenhouse.
380 All other treatments were conducted in a growth cabinet (LPH-411PFQDT-SPC, NK System,
381 Osaka, Japan) with the following environmental conditions: 16 h (28˚C) light/8 h (24˚C) dark at
382 400 μmol photons m^{-2} s^{-1}.
383
384 **$^{15}NH_4$ tracer experiments**
385 The ramet pairs were initially incubated with water for 3 days, followed by a 24-h split treatment
386 with stable isotope-free nitrogen nutrient solutions (2.5 mM NH_4Cl for the +N ramet and the +N
387 split ramet, and 0 mM NH_4Cl for the -N ramet). Roots of the ramets were soaked in 800 mL of 1
388 mM $CaSO_4$ for 1 min to remove the nitrogen treatment solution. The solution for the +N-treated
389 side was then replaced with a solution containing 2.5 mM $^{15}NH_4Cl$ (^{15}N 99 atom%, Shoko
390 Science Co., Ltd., Yokohama, Japan), and $^{15}NH_4^+$ was allowed to be absorbed for 5 min. The
391 roots of ramet pairs were then soaked in 600 mL of 1 mM $CaSO_4$ for 1 min to wash out ^{15}N and
392 then treated again with the stable isotope-free +N or -N hydroponic solutions for 22 h to
393 measure the ammonium absorption activity and for 7 days to measure the absorbed nitrogen
394 distribution with daily changing of the culture solution in a growth cabinet (LPH-411PFQDT-
395 SPC, NK System) with 16 h (30˚C) light/8 h (30˚C) dark at 400 μmol photons m^{-2} s^{-1}.
396 The above-ground tissues, rhizomes, and roots were separately harvested and dried in an
397 oven at 70˚C for at least 5 days. All dried tissues were weighed and ground into fine powders.
398 The ^{15}N and total nitrogen contents were analyzed by Shoko Science Co. with an elemental
399 analyzer-isotope ratio mass spectrometer (Flash2000-DELTA plus Advantage ConFloIII
400 System, Thermo Fisher Scientific, Waltham, MA, United States).

401 The absorption activity of ammonium was calculated as follows. The increase in ^{15}N (μmol)
402 in each sample ($\Delta^{15}N_s$) was calculated from equation (1). W_s, dry weight of the sample (gDW);
403 N_s, the total nitrogen concentration of the sample (%); $^{15}N_s$, the ^{15}N concentration of the sample;
404 and $^{15}N_0$, the naturally occurring ^{15}N concentration (%) of the sample.

405 $$\Delta^{15}N_s = W_s \times 10^6 \times \frac{N_s}{100} \times \frac{^{15}N_s - {}^{15}N_0}{100} \times \frac{1}{15} \qquad (1)$$

406 The $\Delta^{15}N_s$ of each sample (above-ground tissues and roots) were summed to obtain the
407 increase of ^{15}N in the whole ramet pair ($\Delta^{15}N_w$). The absorption activity of ammonium (μmol
408 gDW^{-1} h^{-1}) in roots under +N or +N split conditions was calculated using equation (2). A, the
409 absorption activity of ammonium; W_r, the dry weight of the root that absorbed ^{15}N.

410 $$A = \Delta^{15}N_w \times \frac{1}{W_r} \times \frac{60}{5} \qquad (2)$$

411 The increases in $^{15}N_s$ in each part of the ramet pair ($\Delta^{15}N_s$) were summed to obtain the increase
412 of ^{15}N in the whole ramet pair ($\Delta^{15}N_w$), and the percentage (%) of ^{15}N distributed in each part of
413 the ramet pair was calculated using equation (3). P, the percentage of ^{15}N distributed in each
414 part.

415 $$P = \frac{\Delta^{15}N_s}{\Delta^{15}N_t} \times 100 \qquad (3)$$

416

417 **Reverse transcription-quantitative PCR analysis**

418 Total RNA was extracted from frozen and ground tissues using the RNeasy Plant Mini Kit
419 (Qiagen, Hilden, Germany) with the RNase-Free-DNase Set (Qiagen) according to the
420 supplier's protocols. One μg of total RNA was used to synthesize cDNA using the ReverTra Ace
421 qPCR Master Mix (TOYOBO) according to the supplier's protocol. Twenty-ng cDNA was used
422 for each qPCR reaction with the KAPA SYBR FAST qPCR Master Mix (2X) (KAPA Biosystems,
423 Wilmington, MA, United States) and a real-time PCR system (Applied Biosystems QuantStudio
424 3). Expression levels were estimated using the relative quantification method (Livak and
425 Schmittgen, 2001) with *OlTBC*, a homolog of TBC1 domain family member 22A (Maksup et al.,
426 2013), the internal standard for normalization. Gene locus IDs and the specific primers used for
427 amplification are listed in Supplemental Table S9.

428

429 **Determination of free amino acids**

430 Free amino acids were extracted as described by Konishi et al. (2014). Derivatization of amino
431 acids was carried out using the AccQ-Tag Ultra Derivatization Kit (Waters Corp., Milford, MA,
432 United States). The resulting AccQ-Tag-labeled derivatives were separated and quantified using
433 an HPLC System (Alliance 2695 HPLC system/2475, Waters Corp.) with the AccQTag Column
434 (3.9×150 mm, Waters Corp.) as described in the instruction manual.
435
436 **RNA-Seq analysis**
437 Libraries were prepared with the TruSeq Standard mRNA Library Prep Kit (Illumina, San Diego,
438 CA, United States) using 1 μg of total RNA. Sequence analysis of 40 M reads was performed
439 with a NovaSeq 6000 Sequencing System (Illumina). Library preparation and sequencing were
440 conducted by Macrogen Japan, Inc. (Tokyo). The sequencing reads were mapped to the *O.*
441 *longistaminata* genome obtained from the *Oryza longistaminata* Information Resource
442 (http://olinfres.nig.ac.jp/)(Reuscher et al., 2018) using HISAT2 (Kim et al., 2019), followed by
443 featureCounts (Liao et al., 2014) for counting reads and edgeR (Robinson et al., 2009) for
444 differential expression analysis. Low expression genes were removed using filterByExpr
445 function of edgeR with the default setting. We obtained the presumed function and MAPMAN
446 BIN code for each gene and the presumed corresponding gene ID of *O. sativa* from
447 Supplemental data 2 of Reuscher et al. (2018). Gene ontology (GO) analysis was performed
448 using the corresponding *O. sativa* gene ID list with the analysis tool agriGO
449 (http://systemsbiology.cau.edu.cn/agriGOv2/) (Du et al., 2010; Tian et al., 2017).
450
451 **Growth analysis**
452 Ramet pairs at a similar growth stage were first grown hydroponically in water for 4 days and
453 subsequently exposed to nitrogen split conditions for 5 weeks in a greenhouse using the
454 hydroponic culture solution with (+N split, 2.5 mM NH_4Cl) or without (-N split, 0 mM NH_4Cl)
455 nitrogen. The hydroponic solution was renewed every 3 to 4 days. Growth changes were
456 analyzed at 7-day intervals by measuring plant height, the number of fully expanded leaves, the
457 number of axillary buds growing more than 1 cm, and the chlorophyll content. The chlorophyll
458 content (SPAD value) was measured with a SPAD-502 Plus Chlorophyll Meter (Konica Minolta,
459 Tokyo, Japan) at the tip, middle, and basal parts of leaves, and the average was taken as the

460 SPAD value. For the controls, both ramets of each pair were fed 2.5 mM NH_4Cl (+N) or 0 mM
461 NH_4Cl (-N)-containing hydroponic solution for 5 weeks.
462
463 **Phytohormone quantification**
464 Cytokinins were extracted and semi-purified from about 100 mg fresh weight of root tissues as
465 described previously (Kojima et al., 2009). Cytokinins were quantified using an ultra-
466 performance liquid chromatography (UPLC)-tandem quadrupole mass spectrometer (ACQUITY
467 UPLC System/XEVO-TQXS; Waters Corp.) with an octadecylsilyl (ODS) column (ACQUITY
468 UPLC HSS T3, 1.8 μm, 2.1 mm × 100 mm, Waters Corp.; Kojima et al., 2009).
469
470 **Peptide synthesis**
471 OsCEP1a (DVRHypTNPGHSHypGIGH), OsCEP1b (DVRHypTNHypGHSHypGIGH), OsCEP1c
472 (GVRHypTNPGHSHypGIGH), and OsCEP1d (GVRHypTNHypGHSHypGIGH) were
473 synthesized on a CS 136X synthesizer (CS Bio, Menlo Park, CA, United States) using Fmoc
474 solid phase peptide synthesis chemistry. Hydroxyproline (Hyp) was introduced with Fmoc-
475 Hyp(Boc)-OH purchased from Watanabe Chemical Industries, Ltd. (Hiroshima, Japan). The
476 obtained crude peptides were purified by reverse-phase HPLC on Jasco, Inc. (Tokyo, Japan)
477 preparative instruments with a Jupiter C18 column (5 μm, 300 Å pore size, 21.2 mm internal
478 diameter × 250 mm) (Phenomenex, Torrance, CA, United States), and lyophilized to yield pure
479 peptides.
480
481 **Treatment with synthesized CEP1 peptides**
482 Ramet pairs at a similar growth stage were first grown in hydroponic solution for 3 days in a
483 growth chamber (LPH-411PFQDT-SPC, NK System). Root tips (about 3 cm) from one ramet
484 were removed with a razor blade, and water on the root surface was wiped off with a Kim Towel
485 (Nippon Paper Cresia, Tokyo Japan). The roots were immediately submerged into 100 mL of an
486 ammonium solution containing CEP peptide (+CEPs local: 2.5 mM NH_4Cl, 30 μM of each
487 CEP1a-d). Simultaneously, the root on the other side was submerged in the ammonium solution
488 (systemic: 2.5 mM NH_4Cl) for the indicated period. For the mock control, the roots of each ramet
489 pair were treated with 2.5 mM NH_4Cl.
490

491 **Statistical analysis**

492 Graphs represent the means ± SE of biological-independent experiments. The statistical
493 significance was assayed using means a two-tailed Student's *t*-test or Tukey's honestly
494 significant difference test ($p < 0.05$). The choice of test and the replicate numbers are provided
495 in the corresponding figure legend.

496

497 **Accession numbers**

498 RNA-seq data were deposited to the Gene Expression Omnibus
499 (https://www.ncbi.nlm.nih.gov/geo/) under accession number GSE182486.

500

501 **Supplemental data**

502 The following supplemental materials are available.

503 **Supplemental Figure S1.** The split hydroponic experimental system for *O. longistaminata*
504 ramet pairs.

505 **Supplemental Figure S2.** A Venn diagram showing the overlap among genes up-regulated in
506 the -N treatment compared to the +N treatment, those up-regulated in the -N split treatment
507 compared to +N treatment, and those up-regulated in the +N treatment compared to +N split
508 treatment.

509 **Supplemental Figure S3**. Transcript abundance of *OlNADH-GOGAT1* in the roots of ramet
510 pairs after a 24-h split treatment as measured by RT-qPCR.

511 **Supplemental Table S1.** Genes up-regulated in the +N split treatment compared to the +N
512 treatment

513 **Supplemental Table S2.** Genes up-regulated in the +N treatment compared to the -N treatment

514 **Supplemental Table S3.** Genes up-regulated in the +N treatment compared to the -N split
515 treatment

516 **Supplemental Table S4.** Genes up-regulated in the -N treatment compared to the +N treatment

517 **Supplemental Table S5.** Genes up-regulated in the -N split treatment compared to the +N
518 treatment

519 **Supplemental Table S6.** Genes up-regulated in the +N treatment compared to the +N split
520 treatment

521 **Supplemental Table S7.** Cytokinin concentrations in the roots of +N, +N split, -N split, and -N
522 treated ramets
523 **Supplemental Table S8.** Gene correspondence between *O. sativa* and *O. longistaminata*
524 **Supplemental Table S9.** Primers used for RT-qPCR analysis
525
526 **Acknowledgments**
527 We are grateful to Drs. Motoyuki Ashikari, Tomoyuki Furuta, Takatoshi Kiba, Fanny Bellegarde,
528 Mimi Hashimoto, Shoji Segami (Nagoya University), and Drs. Shinjiro Yamaguchi and Kiyoshi
529 Mashiguchi (Kyoto University) for their helpful support and discussion.
530
531
532
533
534

535 **Figure Legends**

536 **Figure 1.** Compensatory up-regulation of ammonium ion uptake in response to spatially
537 heterogeneous nitrogen availability. A, A schematic representation of the split hydroponic
538 experiment system in which the roots of a ramet pair were separately exposed to independent
539 nitrogen conditions. Details of the experimental design are shown in Fig. S1. B, Compensatory
540 uptake of ammonium ion in +N split roots compared to +N. Ammonium ion uptake activity was
541 measured using $^{15}NH_4^+$ as the tracer. Error bars represent SE of values for biological replicates
542 (n = 3). *$p < 0.05$ (Student's *t*-test). DW, dry weight. C, Accumulation pattern of *OlAMT1;2*
543 transcripts in the roots of *O. longistaminata* ramet pairs after a 24-h split treatment. Transcript
544 abundance, normalized to *OlTBC*, is expressed relative to that of +N, defined as 1. Error bars
545 represent SE of values for biological replicates (n = 3 or 4). Different lowercase letters at the top
546 of each column denote statistically significant differences by Tukey's honestly significant
547 difference test (HSD) ($p < 0.05$).

548

549 **Figure 2.** Transcriptome changes in the roots of ramet pairs in response to spatially
550 heterogeneous nitrogen availability. A, A volcano plot showing differentially expressed genes
551 (FDR < 0.05) between +N and +N split roots. Significantly up-regulated or down-regulated
552 genes in roots from the +N split treatment are shown as red or blue dots, respectively. Numbers
553 in red or blue indicate the total number of up-regulated or down-regulated genes. B, A Venn
554 diagram showing the overlap among the genes up-regulated in the +N split treatment compared
555 to the +N treatment (Up in +N split to +N), those up-regulated in the +N treatment compared to
556 the -N treatment (Up in +N to -N), and those up-regulated in the +N treatment compared to the -
557 N split treatment (Up in +N to -N split). C, The top 20 enriched GO categories among genes up-
558 regulated in the +N split treatment compared to the +N treatment. Highly redundant GO
559 categories were manually removed.

560

561 **Figure 3.** Metabolic responses to spatially heterogeneous nitrogen availability in the roots of *O.*
562 *longistaminata* ramet pairs. A, The expression profile of genes involved in nitrogen assimilation,
563 glycolysis and amino acid biosynthesis. The heatmaps in the pathways were deduced from
564 RNAseq data. Fru1,6-BP, fructose 1,6-bisphosphate; PEP, phospho*enol*-pyruvate; OAA,
565 oxaloacetate; 2OG. 2-oxoglutarate. The details of gene names are provided in Supplemental

566 Table S1. B, Expression patterns of genes analyzed by RT-qPCR. The expression level of each
567 gene, normalized to *OlTBC*, is expressed relative to that of the +N treatment defined as 1. C,
568 Amino acid quantification. The concentrations of amino acids in the roots of each ramet pair
569 after 48 h of split treatment are shown in histograms. Error bars represent the SE of values for
570 biological replicates (n = 3 or 4 for RT-qPCR, and n = 4 for amino acid analysis). Different
571 lowercase letters at the top of each column denote statistically significant differences by Tukey's
572 honestly significant difference test (HSD) ($p < 0.05$).
573
574 **Figure 4.** Allocation of absorbed nitrogen and growth profiles of ramet pairs. A, Distribution of
575 ^{15}N in roots and shoots 7 d after $^{15}NH_4Cl$ feeding. One of the ramets in each split-treated ramet
576 pair was treated with 2.5 mM $^{15}NH_4Cl$ for 5 min and then returned to the normal split treatment.
577 Error bars represent SE of values for biological replicates (n = 3). B to E, Changes in plant
578 height (B, ΔPlant height), number of leaves (C, ΔLeaf number), chlorophyll content (D, ΔSPAD
579 index), and number of growing axillary buds (E, ΔGrowing axl. bud no.) in each ramet after 5
580 weeks of split treatment. Error bars indicate the SE. Different lowercase letters at the top of
581 each column denote statistically significant differences by Tukey's honestly significant difference
582 test (HSD) ($p < 0.05$). n = 6 to 12.
583
584 **Figure 5.** Response of cytokinin and strigolactone biosynthesis to heterogeneous nitrogen
585 conditions. A, Relative expression level of cytokinin biosynthetic genes in ramet roots in
586 response to different nitrogen treatments. Transcript abundance in roots of each ramet after 1
587 week of the split treatment was analyzed by RT-qPCR. B, Cytokinin concentration in the roots of
588 each ramet after 1 week of the split treatment. The complete data set is presented in
589 Supplemental Table S7. tZ, *trans*-zeatin; tZR, tZ riboside; tZRPs, tZR 5'-phosphates; cZ, *cis*-
590 zeatin; cZR, cZ riboside; cZRPs, cZR 5'-phosphates; iP, N^6-(Δ^2-isopentenyl)adenine; iPR, iP
591 riboside; iPRPs, iPR 5'-phosphates; and FW, fresh weight. C, Transcript abundance of
592 strigolactone biosynthetic genes in ramet roots in response to different nitrogen conditions. In
593 (A) and (C), the expression level of each gene normalized by *TBC* is expressed relative to that
594 of the +N treatment defined as 1. Error bars represent the SE of values for biological replicates
595 (n = 4). Different lowercase letters at the top of each column denote statistically significant
596 differences by Tukey's honestly significant difference test (HSD) ($p < 0.05$).

597

598 **Figure 6.** A, Expression pattern of the *O. longistaminata* ortholog of *OsCEP1* (*OlCEP1*) in the
599 roots of ramet pairs after a 24-h split treatment. The expression level of each gene normalized
600 by *TBC* is expressed relative to that of the +N treatment defined as 1. Error bars represent SE
601 of values for biological replicates (n = 3 or 4). Different lowercase letters at the top of each
602 column denote statistically significant differences by Tukey's honestly significant difference test
603 (HSD) ($p < 0.05$). B, Expression of *OlAMT1;2* and *OlGS1;2* genes in the ramet roots in
604 response to exogenously supplied CEP1 peptides. The CEP1 peptide mix was applied to the
605 roots of one of the ramet pairs, and gene expression in the local (+CEP local) and systemic side
606 (systemic) roots after 6 and 24 h treatment was measured. The expression level of each gene,
607 normalized by *TBC*, is expressed relative to that of the +N mock treatment defined as 1. Error
608 bars represent SE of values for biological replicates (n = 3 or 4). *$p < 0.05$ (Student's t-test)
609 compared to the corresponding mock treatment.

610

611

612 **LITERATURE CITED**

613 Alder A, Jamil M, Marzorati M, Bruno M, Vermathen M, Bigler P, Ghisla S, Bouwmeester H,
614 Beyer P, Al-Babili S (2012) The path from β-carotene to carlactone, a strigolactone-like
615 plant hormone. Science 335: 1348–1351
616 Bessho-Uehara K, Nugroho JE, Kondo H, Angeles-Shim RB, Ashikari M (2018) Sucrose affects
617 the developmental transition of rhizomes in Oryza longistaminata. J Plant Res 131: 693–
618 707
619 Chandran AKN, Priatama RA, Kumar V, Xuan Y, Je B Il, Kim CM, Jung KH, Han C deok (2016)
620 Genome-wide transcriptome analysis of expression in rice seedling roots in response to
621 supplemental nitrogen. J Plant Physiol 200: 62–75
622 Davière J-M, Achard P (2017) Organ communication: Cytokinins on the move. Nat Plants 3:
623 17116
624 Delay C, Imin N, Djordjevic MA (2013) CEP genes regulate root and shoot development in
625 response to environmental cues and are specific to seed plants. J Exp Bot 64: 5383–5394
626 Du Z, Zhou X, Ling Y, Zhang Z, Su Z (2010) agriGO: A GO analysis toolkit for the agricultural
627 community. Nucleic Acids Res 38: 64–70
628 Fan Z, Cai Z, Shan J, Yang J (2017) Letter to the Editor: Bud Position and Carbohydrate Play a
629 More Significant Role than Light Condition in the Developmental Transition between
630 Rhizome Buds and Aerial Shoot Buds of Oryza longistaminata. Plant Cell Physiol 58:
631 1281–1282
632 Funayama K, Kojima S, Tabuchi-Kobayashi M, Sawa Y, Nakayama Y, Hayakawa T, Yamaya T
633 (2013) Cytosolic glutamine synthetase1;2 is responsible for the primary assimilation of
634 ammonium in rice roots. Plant Cell Physiol 54: 934–943
635 Gomez-Roldan V, Fermas S, Brewer PB, Puech-Pagès V, Dun EA, Pillot JP, Letisse F,
636 Matusova R, Danoun S, Portais JC, et al (2008) Strigolactone inhibition of shoot
637 branching. Nature 455: 189–194
638 Guo L, Plunkert M, Luo X, Liu Z (2021) Developmental regulation of stolon and rhizome. Curr
639 Opin Plant Biol 59: 101970
640 Ishiyama K, Inoue E, Tabuchi M, Yamaya T, Takahashi H (2004) Biochemical background and
641 compartmentalized functions of cytosolic glutamine synthetase for active ammonium
642 assimilation in rice roots. Plant Cell Physiol 45: 1640–1647
643 Ji Y, Li Q, Liu G, Selvaraj G, Zheng Z, Zou J, Wei Y (2019) Roles of Cytosolic Glutamine
644 Synthetases in Arabidopsis Development and Stress Responses. Plant Cell Physiol 60:
645 657–671
646 Jia Z, von Wirén N (2020) Signaling pathways underlying nitrogen-dependent changes in root
647 system architecture: from model to crop species. J Exp Bot 71: 4393–4404

648 Kamada-Nobusada T, Makita N, Kojima M, Sakakibara H (2013) Nitrogen-dependent regulation
649 of de novo cytokinin biosynthesis in rice: The role of glutamine metabolism as an
650 additional signal. Plant Cell Physiol 54: 1881–1893
651 Kiba T, Takei K, Kojima M, Sakakibara H (2013) Side-Chain Modification of Cytokinins Controls
652 Shoot Growth in Arabidopsis. Dev Cell 27: 452–461
653 Kim D, Paggi JM, Park C, Bennett C, Salzberg SL (2019) Graph-based genome alignment and
654 genotyping with HISAT2 and HISAT-genotype. Nat Biotechnol 37: 907–915
655 Kojima M, Kamada-Nobusada T, Komatsu H, Takei K, Kuroha T, Mizutani M, Ashikari M,
656 Ueguchi-Tanaka M, Matsuoka M, Suzuki K, et al (2009) Highly sensitive and high-
657 throughput analysis of plant hormones using ms-probe modification and liquid
658 chromatographytandem mass spectrometry: An application for hormone profiling in oryza
659 sativa. Plant Cell Physiol 50: 1201–1214
660 De Kroon H, Van Der Zalm E, Van Rheenen JWA, Van Dijk A, Kreulen R (1998) The interaction
661 between water and nitrogen translocation in a rhizomatous sedge (Carex flacca).
662 Oecologia 116: 38–49
663 Kyozuka J (2017) Letter to the Editor: Author Response - Analysis of Rhizome Development in
664 Oryza longistaminata, a Wild Rice Species. Plant Cell Physiol 58: 1283
665 Landrein B, Formosa-Jordan P, Malivert A, Schuster C, Melnyk CW, Yang W, Turnbull C,
666 Meyerowitz EM, Locke JCW, Jönsson H (2018) Nitrate modulates stem cell dynamics in
667 Arabidopsis shoot meristems through cytokinins. Proc Natl Acad Sci U S A 115: 1382–
668 1387
669 Lea PJ, Miflin BJ (1974) Alternative route for nitrogen assimilation in higher plants. 251: 614–
670 616
671 Lee S, Marmagne A, Park J, Fabien C, Yim Y, Kim S ji, Kim TH, Lim PO, Masclaux-Daubresse
672 C, Nam HG (2020a) Concurrent activation of OsAMT1;2 and OsGOGAT1 in rice leads to
673 enhanced nitrogen use efficiency under nitrogen limitation. Plant J 103: 7–20
674 Lee S, Park J, Lee J, Shin D, Marmagne A, Lim PO, Masclaux-Daubresse C, An G, Nam HG
675 (2020b) OsASN1 overexpression in rice increases grain protein content and yield under
676 nitrogen-limiting conditions. Plant Cell Physiol 61: 1309–1320
677 Li C, Tang Z, Wei J, Qu H, Xie Y, Xu G (2016) The OsAMT1.1 gene functions in ammonium
678 uptake and ammonium–potassium homeostasis over low and high ammonium
679 concentration ranges. J Genet Genomics 43: 639–649
680 Liao Y, Smyth GK, Shi W (2014) FeatureCounts: An efficient general purpose program for
681 assigning sequence reads to genomic features. Bioinformatics 30: 923–930
682 Livak KJ, Schmittgen TD (2001) Analysis of relative gene expression data using real-time
683 quantitative PCR and the 2-ΔΔCT method. Methods 25: 402–408

684 Maeda Y, Konishi M, Kiba T, Sakuraba Y, Sawaki N, Kurai T, Ueda Y, Sakakibara H,
685 Yanagisawa S (2018) A NIGT1-centred transcriptional cascade regulates nitrate signalling
686 and incorporates phosphorus starvation signals in Arabidopsis. Nat Commun 9: 1376
687 Maksup S, Supaibulwatana K, Selvaraj G (2013) High-quality reference genes for quantifying
688 the transcriptional responses of Oryza sativa L. (ssp. indica and japonica) to abiotic stress
689 conditions. Chinese Sci Bull 58: 1919–1930
690 Minakuchi K, Kameoka H, Yasuno N, Umehara M, Luo L, Kobayashi K, Hanada A, Ueno K,
691 Asami T, Yamaguchi S, et al (2010) FINE CULM1 (FC1) works downstream of
692 strigolactones to inhibit the outgrowth of axillary buds in rice. Plant Cell Physiol 51: 1127–
693 1135
694 Naulin PA, Armijo GI, Vega AS, Tamayo KP, Gras DE, De La Cruz J, Gutiérrez RA (2019)
695 Nitrate Induction of Primary Root Growth Requires Cytokinin Signaling in Arabidopsis
696 thaliana. Plant Cell Physiol 61: 342–352
697 Nishida H, Suzaki T (2018) Two Negative Regulatory Systems of Root Nodule Symbiosis: How
698 Are Symbiotic Benefits and Costs Balanced? Plant Cell Physiol 59: 1733–1738
699 Ohashi M, Ishiyama K, Kojima S, Kojima M, Sakakibara H, Yamaya T, Hayakawa T (2017) Lack
700 of cytosolic glutamine synthetase1;2 activity reduces nitrogen-dependent biosynthesis of
701 cytokinin required for axillary bud outgrowth in rice seedlings. Plant Cell Physiol 58: 679–
702 690
703 Ohkubo Y, Kuwata K, Matsubayashi Y (2021) A type 2C protein phosphatase activates high-
704 affinity nitrate uptake by dephosphorylating NRT2.1. Nat Plants 7: 310–316
705 Ohkubo Y, Tanaka M, Tabata R, Ogawa-Ohnishi M, Matsubayashi Y (2017) Shoot-to-root
706 mobile polypeptides involved in systemic regulation of nitrogen acquisition. Nat Plants 3:
707 17029
708 Ohyama K, Ogawa M, Matsubayashi Y (2008) Identification of a biologically active, small,
709 secreted peptide in Arabidopsis by in silico gene screening, followed by LC-MS-based
710 structure analysis. Plant J 55: 152–160
711 Okamoto S, Tabata R, Matsubayashi Y (2016) Long-distance peptide signaling essential for
712 nutrient homeostasis in plants. Curr Opin Plant Biol 34: 35–40
713 Osugi A, Kojima M, Takebayashi Y, Ueda N, Kiba T, Sakakibara H (2017) Systemic transport of
714 trans-zeatin and its precursor have differing roles in Arabidopsis shoots. Nat Plants. doi:
715 10.1038/nplants.2017.112
716 Ota R, Ohkubo Y, Yamashita Y, Ogawa-Ohnishi M, Matsubayashi Y (2020) Shoot-to-root
717 mobile CEPD-like 2 integrates shoot nitrogen status to systemically regulate nitrate uptake
718 in Arabidopsis. Nat Commun 11: 641

719 Ravazzolo L, Boutet-Mercey S, Perreau F, Forestan C, Varotto S, Ruperti B, Quaggiotti S
720 (2021) Strigolactones and Auxin Cooperate to Regulate Maize Root Development and
721 Response to Nitrate. Plant Cell Physiol 0: 1–14
722 Ravazzolo L, Trevisan S, Manoli A, Boutet-Mercey S, Perreau F, Quaggiotti S (2019) The
723 Control of Zealactone Biosynthesis and Exudation is Involved in the Response to Nitrogen
724 in Maize Root. Plant Cell Physiol 60: 2100–2112
725 Reuscher S, Furuta T, Bessho-Uehara K, Cosi M, Jena KK, Toyoda A, Fujiyama A, Kurata N,
726 Ashikari M (2018) Assembling the genome of the African wild rice Oryza longistaminata by
727 exploiting synteny in closely related Oryza species. Commun Biol 1: 162
728 Robinson MD, McCarthy DJ, Smyth GK (2009) edgeR: A Bioconductor package for differential
729 expression analysis of digital gene expression data. Bioinformatics 26: 139–140
730 Ruffel S (2018) Nutrient-Related Long-Distance Signals: Common Players and Possible Cross-
731 Talk. Plant Cell Physiol 59: 1723–1732
732 Ruffel S, Gojon A (2017) Systemic nutrient signalling: On the road for nitrate. Nat Plants 3: 1–2
733 Sakakibara H (2021) Cytokinin biosynthesis and transport for systemic nitrogen signaling. Plant
734 J 105: 421–430
735 Sakakibara H, Takei K, Hirose N (2006) Interactions between nitrogen and cytokinin in the
736 regulation of metabolism and development. Trends Plant Sci 11: 440–448
737 Scheible WR, González-Fontes A, Lauerer M, Müller-Röber B, Caboche M, Stitt M (1997)
738 Nitrate acts as a signal to induce organic acid metabolism and repress starch metabolism
739 in tobacco. Plant Cell 9: 783–798
740 Scheible WR, Morcuende R, Czechowski T, Fritz C, Osuna D, Palacios-Rojas N, Schindelasch
741 D, Thimm O, Udvardi MK, Stitt M (2004) Genome-wide reprogramming of primary and
742 secondary metabolism, protein synthesis, cellular growth processes, and the regulatory
743 infrastructure of arabidopsis in response to nitrogen. Plant Physiol 136: 2483–2499
744 Shibasaki K, Takebayashi A, Makita N, Kojima M, Takebayashi Y, Kawai M, Hachiya T,
745 Sakakibara H (2021) Nitrogen Nutrition Promotes Rhizome Bud Outgrowth via Regulation
746 of Cytokinin Biosynthesis Genes and an Oryza longistaminata Ortholog of FINE CULM 1.
747 Front Plant Sci 12: 670101
748 Sonoda Y, Ikeda A, Saiki S, Von Wirén N, Yamaya T, Yamaguchi J (2003) Distinct expression
749 and function of three ammonium transporter genes (OsAMT1;1 - 1;3) in rice. Plant Cell
750 Physiol 44: 726–734
751 Suenaga A, Moriya K, Sonoda Y, Ikeda A, Von Wirén N, Hayakawa T, Yamaguchi J, Yamaya T
752 (2003) Constitutive expression of a novel-type ammonium transporter OsAMT2 in rice
753 plants. Plant Cell Physiol 44: 206–211

754 Sui Z, Wang T, Li H, Zhang M, Li Y, Xu R, Xing G, Ni Z, Xin M (2016) Overexpression of
755 peptide-encoding OsCEP6.1 results in pleiotropic effects on growth in rice (O. sativa).
756 Front Plant Sci 7: 1–12
757 Sun H, Tao J, Liu S, Huang S, Chen S, Xie X, Yoneyama K, Zhang Y, Xu G (2014)
758 Strigolactones are involved in phosphate- and nitrate-deficiency-induced root development
759 and auxin transport in rice. J Exp Bot 65: 6735–6746
760 Sun L, Di DW, Li G, Li Y, Kronzucker HJ, Shi W (2020) Transcriptome analysis of rice (Oryza
761 sativa L.) in response to ammonium resupply reveals the involvement of phytohormone
762 signaling and the transcription factor OsJAZ9 in reprogramming of nitrogen uptake and
763 metabolism. J Plant Physiol 246–247: 153137
764 Tabata R, Sumida K, Yoshii T, Ohyama K, Shinohara H, Matsubayashi Y (2014) Perception of
765 root-derived peptides by shoot LRR-RKs mediates systemic N-demand signaling. Science
766 (80-) 346: 343–346
767 Tabuchi M, Abiko T, Yamaya T (2007) Assimilation of ammonium ions and reutilization of
768 nitrogen in rice (Oryza sativa L.). J Exp Bot 58: 2319–2327
769 Tabuchi M, Sugiyama K, Ishiyama K, Inoue E, Sato T, Takahashi H, Yamaya T (2005) Severe
770 reduction in growth rate and grain filling of rice mutants lacking OsGS1;1, a cytosolic
771 glutamine synthetase1;1. Plant J 42: 641–651
772 Takei K, Ueda N, Aoki K, Kuromori T, Hirayama T, Shinozaki K, Yamaya T, Sakakibara H
773 (2004) AtIPT3 is a key determinant of nitrate-dependent cytokinin biosynthesis in
774 Arabidopsis. Plant Cell Physiol 45: 1053–1062
775 Tian T, Liu Y, Yan H, You Q, Yi X, Du Z, Xu W, Su Z (2017) AgriGO v2.0: A GO analysis toolkit
776 for the agricultural community, 2017 update. Nucleic Acids Res 45: W122–W129
777 Toriba T, Tokunaga H, Nagasawa K, Nie F, Yoshida A, Kyozuka J (2020) Suppression of Leaf
778 Blade Development by BLADE-ON-PETIOLE Orthologs Is a Common Strategy for
779 Underground Rhizome Growth. Curr Biol 30: 509-516.e3
780 Umehara M, Hanada A, Magome H, Takeda-Kamiya N, Yamaguchi S (2010) Contribution of
781 strigolactones to the inhibition of tiller bud outgrowth under phosphate deficiency in rice.
782 Plant Cell Physiol 51: 1118–1126
783 Umehara M, Hanada A, Yoshida S, Akiyama K, Arite T, Takeda-Kamiya N, Magome H, Kamiya
784 Y, Shirasu K, Yoneyama K, et al (2008) Inhibition of shoot branching by new terpenoid
785 plant hormones. Nature 455: 195–200
786 Vaughan DA (1994) The Wild Relatives of Rice: A Genetic Resources Handbook. IRRI, Los
787 Banos

788 Wang R, Tischner R, Gutiérrez RA, Hoffman M, Xing X, Chen M, Coruzzi G, Crawford NM
789 (2004) Genomic analysis of the nitrate response using a nitrate reductase-null mutant of
790 arabidopsis. Plant Physiol 136: 2512–2522
791 Wheeldon CD, Bennett T (2021) There and back again: An evolutionary perspective on long-
792 distance coordination of plant growth and development. Semin Cell Dev Biol 109: 55–67
793 Xiong D, Yu T, Ling X, Fahad S, Peng S, Li Y, Huang J (2015) Sufficient leaf transpiration and
794 nonstructural carbohydrates are beneficial for high-temperature tolerance in three rice
795 (Oryza sativa) cultivars and two nitrogen treatments. Funct Plant Biol 42: 347–356
796 Xu J, Zha M, Li Y, Ding Y, Chen L, Ding C, Wang S (2015) The interaction between nitrogen
797 availability and auxin, cytokinin, and strigolactone in the control of shoot branching in rice
798 (Oryza sativa L.). Plant Cell Rep 34: 1647–1662
799 Yamaya T, Kusano M (2014) Evidence supporting distinct functions of three cytosolic glutamine
800 synthetases and two NADH-glutamate synthases in rice. J Exp Bot 65: 5519–5525
801 Yang HC, Kan CC, Hung TH, Hsieh PH, Wang SY, Hsieh WY, Hsieh MH (2017) Identification of
802 early ammonium nitrate-responsive genes in rice roots. Sci Rep 7: 1–16
803 Yoshida A, Terada Y, Toriba T, Kose K, Ashikari M, Kyozuka J (2016) Analysis of rhizome
804 development in oryza longistaminata, a wild rice species. Plant Cell Physiol 57: 2213–
805 2220
806 Yoshida S (1981) Mineral nutrition of rice. Fundam. rice Crop Sci. International Rice Research
807 Institute, Los Banos, Philippines, pp 111–176
808 Yuan L, Loqué D, Kojima S, Rauch S, Ishiyama K, Inoue E, Takahashi H, Wirén, von N (2007)
809 The organization of high-affinity ammonium uptake in Arabidopsis roots depends on the
810 spatial arrangement and biochemical properties of AMT1-type transporters. Plant Cell 19:
811 2636–2652
812
813

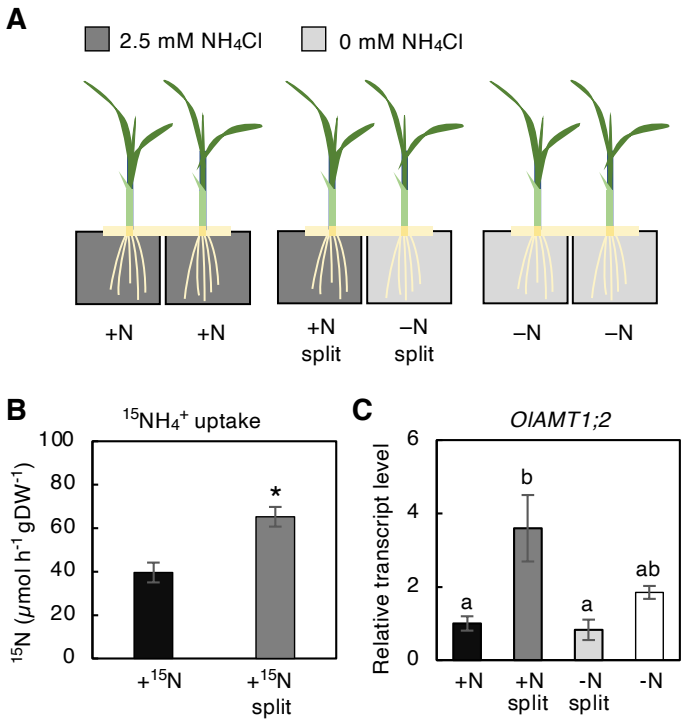

Figure 1. Compensatory up-regulation of ammonium ion uptake in response to spatially heterogeneous nitrogen availability. A, A schematic representation of the split hydroponic experiment system in which the roots of a ramet pair were separately exposed to independent nitrogen conditions. Details of the experimental design are shown in Fig. S1. B, Compensatory uptake of ammonium ion in +N split roots compared to +N. Ammonium ion uptake activity was measured using $^{15}NH_4^+$ as the tracer. Error bars represent SE of values for biological replicates (n = 3). *$p < 0.05$ (Student's *t*-test). DW, dry weight. C, Accumulation pattern of *OlAMT1;2* transcripts in the roots of *O. longistaminata* ramet pairs after a 24-h split treatment. Transcript abundance, normalized to *OlTBC*, is expressed relative to that of +N, defined as 1. Error bars represent SE of values for biological replicates (n = 3 or 4). Different lowercase letters at the top of each column denote statistically significant differences by Tukey's honestly significant difference test (HSD) ($p < 0.05$).

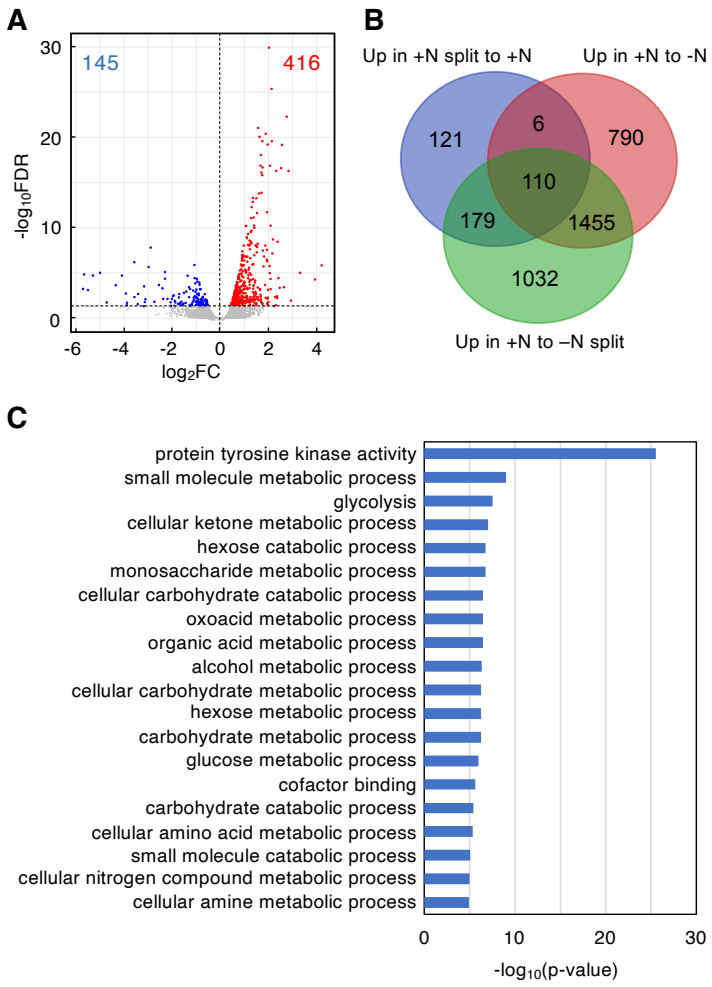

Figure 2. Transcriptome changes in the roots of ramet pairs in response to spatially heterogeneous nitrogen availability. A, A volcano plot showing differentially expressed genes (FDR < 0.05) between +N and +N split roots. Significantly up-regulated or down-regulated genes in roots from the +N split treatment are shown as red or blue dots, respectively. Numbers in red or blue indicate the total number of up-regulated or down-regulated genes. B, A Venn diagram showing the overlap among the genes up-regulated in the +N split treatment compared to the +N treatment (Up in +N split to +N), those up-regulated in the +N treatment compared to the -N treatment (Up in +N to -N), and those up-regulated in the +N treatment compared to the -N split treatment (Up in +N to -N split). C, The top 20 enriched GO categories among genes up-regulated in the +N split treatment compared to the +N treatment. Highly redundant GO categories were manually removed.

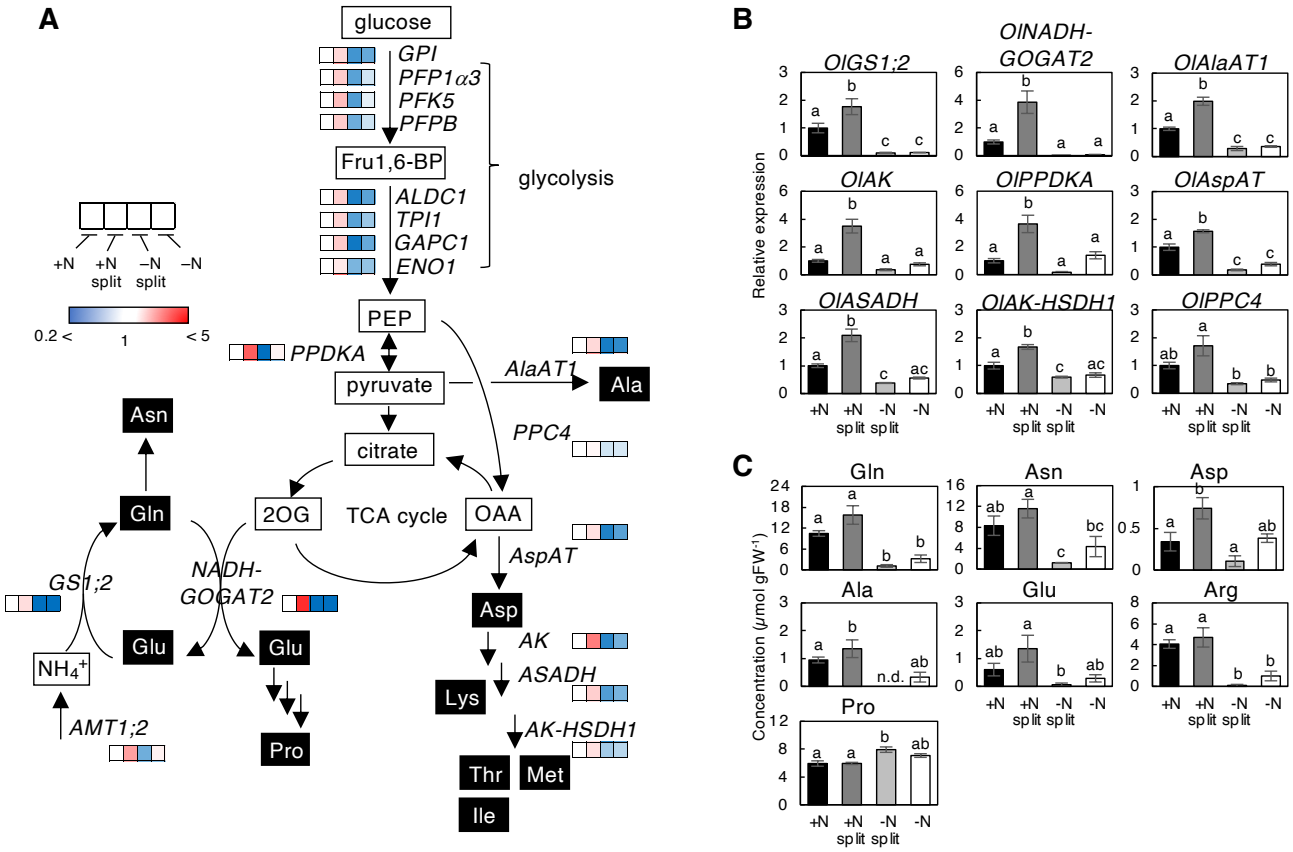

Figure 3. Metabolic responses to spatially heterogeneous nitrogen availability in the roots of *O. longistaminata* ramet pairs. A, The expression profile of genes involved in nitrogen assimilation, glycolysis and amino acid biosynthesis. The heatmaps in the pathways were deduced from RNAseq data. Fru1,6-BP, fructose 1,6-bisphosphate; PEP, phospho*enol*-pyruvate; OAA, oxaloacetate; 2OG. 2-oxoglutarate. The details of gene names are provided in Supplemental Table S1. B, Expression patterns of genes analyzed by RT-qPCR. The expression level of each gene, normalized to *OlTBC*, is expressed relative to that of the +N treatment defined as 1. C, Amino acid quantification. The concentrations of amino acids in the roots of each ramet pair after 48 h of split treatment are shown in histograms. Error bars represent the SE of values for biological replicates (n = 3 or 4 for RT-qPCR, and n = 4 for amino acid analysis). Different lowercase letters at the top of each column denote statistically significant differences by Tukey's honestly significant difference test (HSD) ($p < 0.05$).

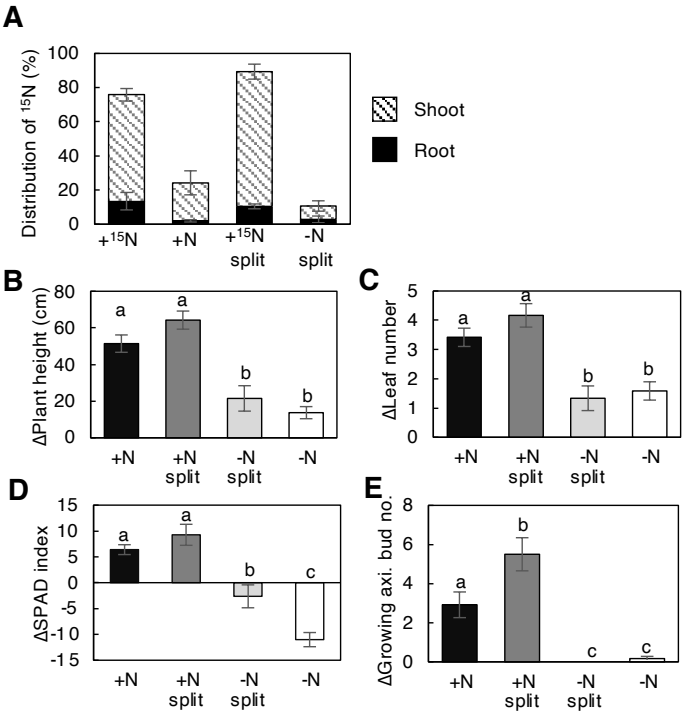

Figure 4. Allocation of absorbed nitrogen and growth profiles of ramet pairs. A, Distribution of ^{15}N in roots and shoots 7 d after $^{15}NH_4Cl$ feeding. One of the ramets in each split-treated ramet pair was treated with 2.5 mM $^{15}NH_4Cl$ for 5 min and then returned to the normal split treatment. Error bars represent SE of values for biological replicates (n = 3). B to E, Changes in plant height (B, ΔPlant height), number of leaves (C, ΔLeaf number), chlorophyll content (D, ΔSPAD index), and number of growing axillary buds (E, ΔGrowing axl. bud no.) in each ramet after 5 weeks of split treatment. Error bars indicate the SE. Different lowercase letters at the top of each column denote statistically significant differences by Tukey's honestly significant difference test (HSD) ($p < 0.05$). n = 6 to 12.

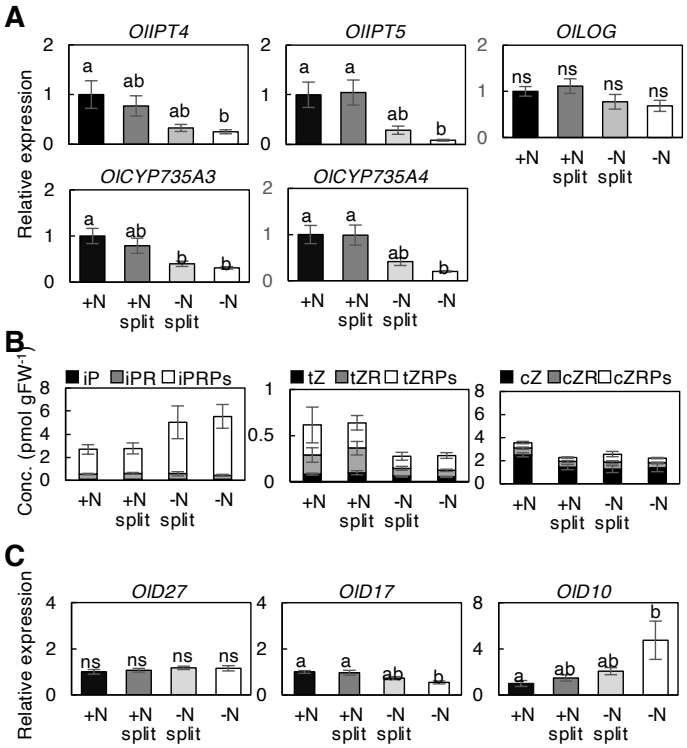

Figure 5. Response of cytokinin and strigolactone biosynthesis to heterogeneous nitrogen conditions. A, Relative expression level of cytokinin biosynthetic genes in ramet roots in response to different nitrogen treatments. Transcript abundance in roots of each ramet after 1 week of the split treatment was analyzed by RT-qPCR. B, Cytokinin concentration in the roots of each ramet after 1 week of the split treatment. The complete data set is presented in Supplemental Table S8. tZ, *trans*-zeatin; tZR, tZ riboside; tZRPs, tZR 5'-phosphates; cZ, *cis*-zeatin; cZR, cZ riboside; cZRPs, cZR 5'-phosphates; iP, N^6-(Δ^2-isopentenyl)adenine; iPR, iP riboside; iPRPs, iPR 5'-phosphates; and FW, fresh weight. C, Transcript abundance of strigolactone biosynthetic genes in ramet roots in response to different nitrogen conditions. In (A) and (C), the expression level of each gene normalized by *TBC* is expressed relative to that of the +N treatment defined as 1. Error bars represent the SE of values for biological replicates (n = 4). Different lowercase letters at the top of each column denote statistically significant differences by Tukey's honestly significant difference test (HSD) ($p < 0.05$).

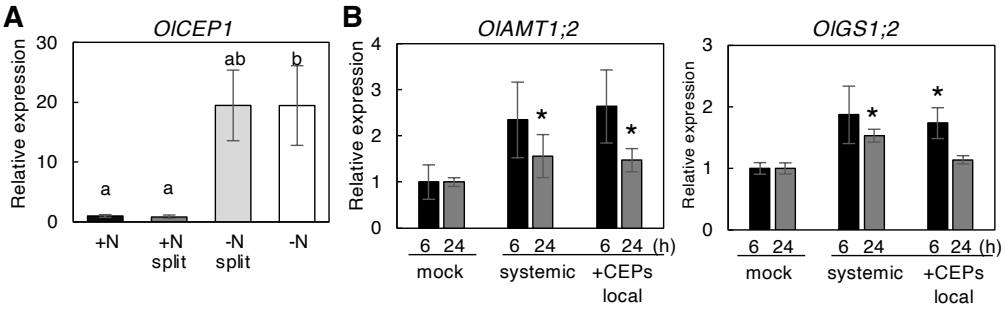

Figure 6. A, Expression pattern of the *O. longistaminata* ortholog of *OsCEP1* (*OlCEP1*) in the roots of ramet pairs after a 24-h split treatment. The expression level of each gene normalized by *TBC* is expressed relative to that of the +N treatment defined as 1. Error bars represent SE of values for biological replicates (n = 3 or 4). Different lowercase letters at the top of each column denote statistically significant differences by Tukey's honestly significant difference test (HSD) ($p < 0.05$). B, Expression of *OlAMT1;2* and *OlGS1;2* genes in the ramet roots in response to exogenously supplied CEP1 peptides. The CEP1 peptide mix was applied to the roots of one of the ramet pairs, and gene expression in the local (+CEP local) and systemic side (systemic) roots after 6 and 24 h treatment was measured. The expression level of each gene, normalized by *TBC*, is expressed relative to that of the +N mock treatment defined as 1. Error bars represent SE of values for biological replicates (n = 3 or 4). *$p < 0.05$ (Student's t-test) compared to the corresponding mock treatment.

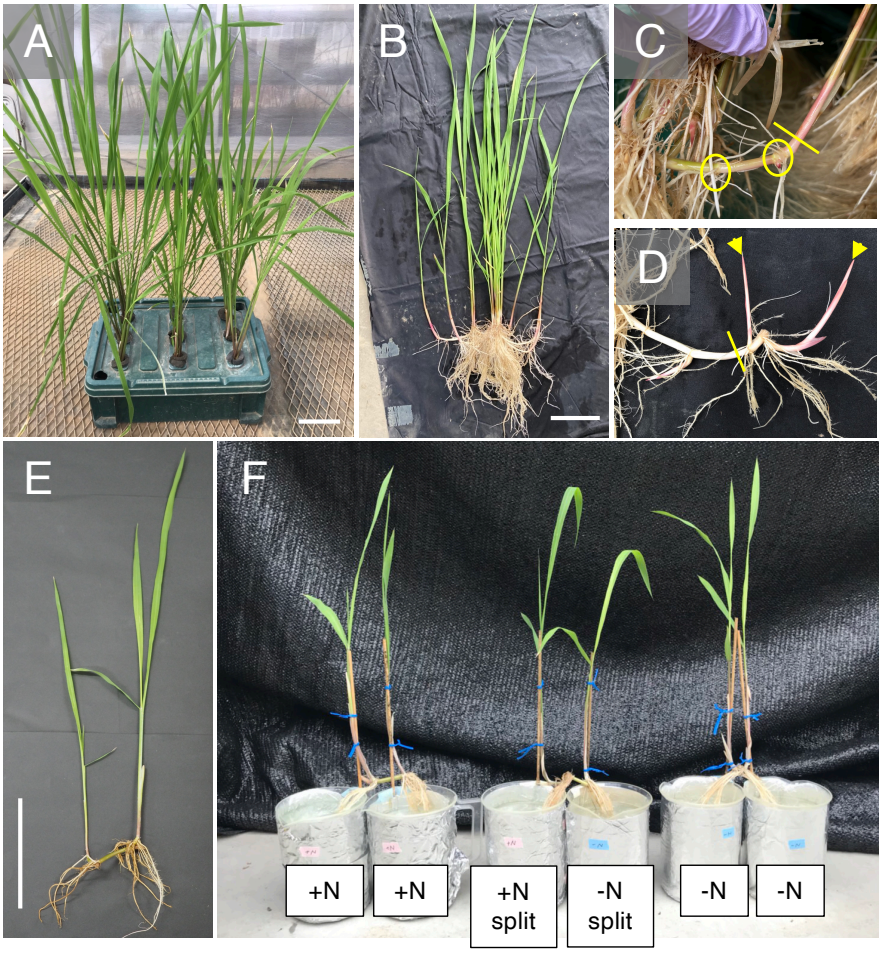

Supplemental Figure S1. The split hydroponic experimental system for *O. longistaminata* ramet pairs. A, *O. longistaminata* hydroponic culture. The plants were maintained in a 10 L-container. Scale bar, 10 cm. B, A clonal colony of *O. longistaminata*. Scale bar, 10 cm. C, A rhizome grown in the hydroponic culture. Ovals identify adjacent nodes. The tip of a primary rhizome was cut at the yellow line to induce the outgrowth of secondary rhizomes. D, Growth of secondary rhizomes at adjacent nodes (arrowheads). The pair was excised from the parental colony at the yellow line for further growth. E, A ramet pair grown from adjacent rhizome nodes. Scale bar, 15 cm. F, Split treatments with different nitrogen conditions. Each pot contains 1 L of nutrient solution.

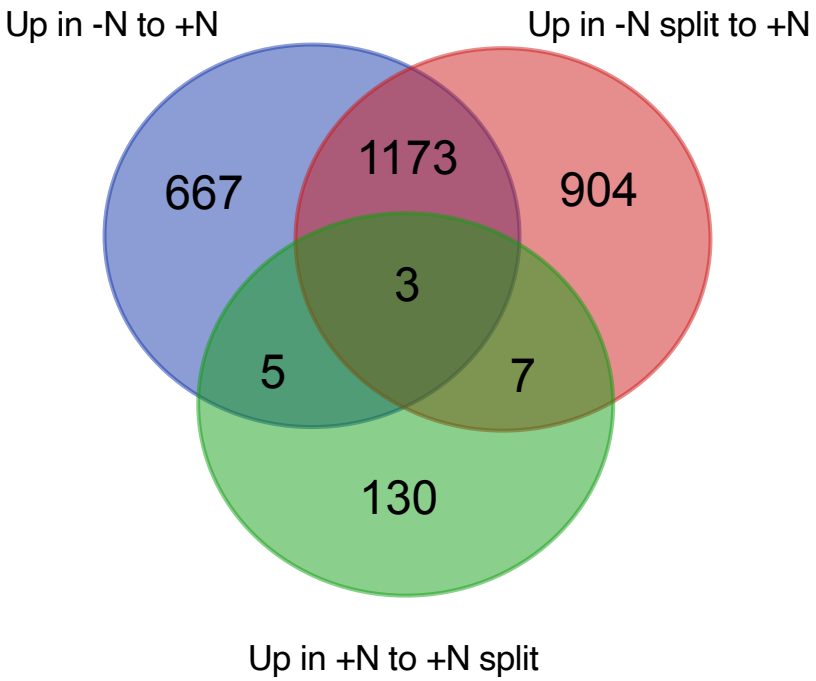

Supplemental Figure S2. A Venn diagram showing the overlap among genes up-regulated in the -N treatment compared to the +N treatment (Up in -N to +N), those up-regulated in the -N split treatment compared to +N treatment (Up in -N split to +N), and those up-regulated in the +N treatment compared to +N split treatment (Up in +N to +N split).

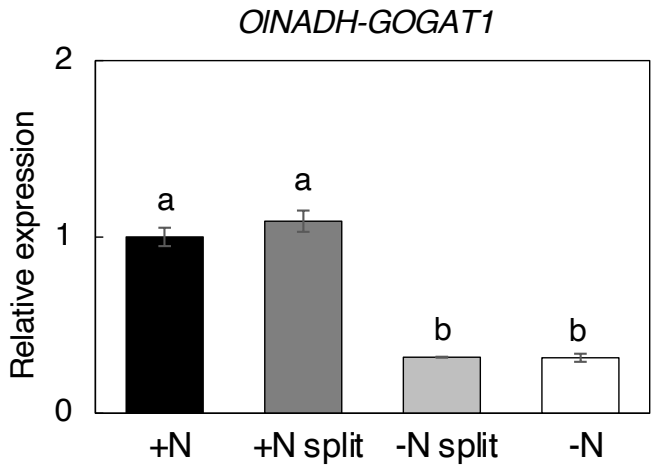

Supplemental Figure S3. Transcript abundance of *OlNADH-GOGAT1* in the roots of ramet pairs after a 24-h split treatment as measured by RT-qPCR. The expression level of each gene, normalized by *TBC*, is expressed relative to that of the +N treatment defined as 1. Error bars represent SE of values for biological replicates (n = 3 or 4). Different lowercase letters at the top of each column denote statistically significant differences by Tukey's honestly significant difference test (HSD) ($p < 0.05$).